Three-Dimensional Microtumors for Probing Heterogeneity of Invasive Bladder Cancer

Peter Torab[1,#], Yue Yan[2,#], Hironobu Yamashita[3], Joshua I. Warrick[3,4], Jay D. Raman[4], David J. DeGraff[3,4,5], and Pak Kin Wong[1,2,4,*]

[1]Department of Mechanical Engineering, The Pennsylvania State University, 137 Reber Building, University Park, PA 16802

[2]Department of Biomedical Engineering, The Pennsylvania State University, 122 Chemical and Biomedical Engineering Building, University Park, PA 16802

[3]Department of Pathology and Laboratory Medicine, Penn State Health Milton S. Hershey Medical Center, 500 University Dr, Hershey, PA 17033

[4]Department of Surgery, Division of Urology, Penn State Health Milton S. Hershey Medical Center, 200 Campus Dr, Hershey, PA 17033

[5]Department of Biochemistry and Molecular Biology, Penn State Health Milton S. Hershey Medical Center, 400 University Drive, Hershey, PA 17033

#These authors contribute equally

*Corresponding author: pak@engr.psu.edu, +1-814-863-5267

Abstract

Bladder cancer is an increasingly common malignancy, and muscle invasive bladder cancer is associated with particularly high rates of morbidity and mortality. The morphologic and molecular diversity of bladder cancer poses significant challenges in elucidating the invasion mechanisms responsible for disease progression. Furthermore, conventional invasion assays do not provide a physiological context for studying bladder cancer invasion within 3D microenvironments and have limited ability to capture the contribution of cellular phenotypic heterogeneity to disease progression. Here, we describe the development of a 3D microtumor invasion model suitable for the analysis of cellular phenotypic heterogeneity in cell lines and primary tumor cells from bladder cancer patients. This model incorporates a self-assembly approach for recapitulating features of bladder cancer invasion in 3D microenvironments and probing the invasive cell subpopulations. The gene expression profiles of invading microtumors were analyzed by incorporating a gold nanorod-locked nucleic acid biosensor. Incorporation of the single cell biosensor and transient gene knockdown into the system revealed the formation of invasive leader cells with upregulated Delta-like ligand 4 (DLL4) expression, as well as the role of NOTCH1-DLL4 signaling in collective bladder cancer invasion. The involvement of DLL4 expressing cells in bladder cancer invasion was also observed in patient samples obtained from transurethral resection. Collectively, our study demonstrates a 3D microtumor invasion model for investigating intracellular heterogeneity of bladder cancer invasion and analyzing patient derived samples toward personalized medicine applications.

Bladder cancer is the second most common genitourinary malignancy in the United States and is associated with high treatment costs and poor patient outcomes. Early stage or non-muscle invasive disease (tumor stage ≤ T1) is often recurrent and manifests occasionally with progression to locally advanced or muscle invasive disease (Figure 1A). In contrast, advanced bladder cancer is especially lethal, as the five-year survival rates of patients diagnosed with stages T2 and T3 diseases are ~63% and ~46% [1]. In addition, ~50% of muscle invasive bladder cancer patients experience disease recurrence, usually in the form of metastatic disease which is almost uniformly lethal.

Histological studies and molecular subtyping have revealed that bladder cancer is a complex malignancy with heterogeneous characteristics at the molecular and cellular levels.[1–3] Due to the molecular diversity and complexity of the disease, it is challenging to identify which bladder cancer patients are at the greatest risk for disease recurrence and progression and death.[4] Molecular characterization of tumors has the potential to better identify the inherent phenotypic behavior of bladder cancers not entirely captured with standard pathologic analysis. In this regard, several groups have independently completed a molecular characterization of human bladder cancer, leading to the discovery of several transcriptional subtypes of muscle invasive bladder cancer.[5–7] One specific subtype, referred to as "luminal", exhibits a transcriptional profile with expression hallmarks similar to that of the normal luminal urothelium. Luminal bladder cancers typically present with the morphology of urothelial carcinoma. However, another transcriptional subtype referred to as "basal" is frequently observed in bladder cancer cells that have undergone squamous metaplasia/differentiation. Basal bladder cancer is one of the most aggressive bladder cancer subtypes described to date.[6] While these and other transcriptional subtypes (and associated morphologies) were originally identified at the patient-population level, it is now clear that luminal and basal molecular subtypes can co-exist within an individual tumor.[8,9] However, it is unknown

how (or if) these elements of tumor heterogeneity contribute to disease pathogenesis in general, and invasiveness in particular.

Recently, 3D organoid and tissue-engineered models have emerged as a more physiologically relevant alternative to traditional 2D adherent cell models.[10–12] Several approaches have also been developed to study tumor cell invasion through the extracellular matrix (ECM) in vitro. These approaches include spheroid sprouting assays,[13] modified Boyden chambers,[14,15] and microfluidic culture systems.[16] Nevertheless, conventional invasion assays often focus on the invasion of cancer cells at the population level and pay little attention to the behaviors of subpopulations and individual cells within a given population. The influence of cellular and molecular heterogeneity on bladder cancer invasion remains poorly understood. Furthermore, the collective invasion mechanisms, such as the formation of invasive leader cells,[17] have not been investigated systematically in bladder cancer. The investigation of 3D tumor invasion is further hampered by the lack of effective approaches to dynamically monitor gene expression in 3D microenvironments. This is particularly challenging for characterizing the molecular diversity in human patient-derived tumor samples. The lack of an effective bladder cancer invasion assay, therefore, has limited the investigation of the invasion mechanisms and the innovation in the clinical management of this common disease.

In this study, we developed a tumor bioengineering strategy to study invading microtumors in 3D microenvironments. In particular, multifocal microtumor structures were self-assembled on ECM by urothelial carcinoma cells to model the stratified urothelium including the basement membrane. Using established human bladder cancer cells with basal and luminal molecular features,[18] we investigated their invasiveness in the 3D invasion assay. We also characterized the invasive subpopulations that displayed aggressive behaviors within the population. We additionally explored the existence of invasive leader

cells, which have been shown in other models but not bladder cancer.[19] Microtumor constituent single cell gene expression analysis with gold nanorod locked nucleic acid (GNR-LNA) biosensors[20–22] was used to evaluate the expression of delta-like ligand 4 (DLL4), which regulates tip cell formation during angiogenesis[23,24] and leader cell formation during epithelial wound healing.[25,26] Transient knockdown and pharmacological perturbation experiments were performed to modulate DLL4 expression, and the resulting effects on tumor invasion were monitored. The results indicated that NOTCH1-DLL4 signaling plays an important role in collective invasion of bladder cancer, as DLL4 was upregulated in invasive tumor spheroids, particularly at the invading front. Human clinical specimens derived from transurethral resection of bladder tumors (TURBT) were applied to study the compatibility of the model with primary cells. DLL4 expression was similarly upregulated in the primary cell spheroid and detached cell aggregates. Overall, the 3D microtumor assay enables molecular-focused studies related to tumor heterogeneity and its role in bladder cancer progression.

Experimental Section

Cell Culture of Established Urothelial Cancer Cell Lines

The bladder cancer cell lines RT4, UM-UC-3, and HT-1376 were obtained from ATCC, and UM-UC-1 was obtained from Sigma-Aldrich. Upper tract urothelial carcinoma cell lines CRL-9520 and UM-UC-14 were obtained from ATCC and Sigma-Aldrich, respectively. RT4 cells were maintained in McCoy's 5A culture medium, CRL-9520 was maintained in F-12K, and all other cell lines were maintained in MEM with 2 mM glutamine (Corning). Culture medium for HT-1376 was supplemented with 1x non-essential amino acids and 1 mM sodium pyruvate (Gibco). All culture media were supplemented with 10% fetal bovine serum (Corning) and 1 μg/mL Gentamicin (Gibco). The effects of cell culture media on invasion were not considered in this study. Cells were grown in 60 mm tissue culture dishes and were incubated at 37°C, 5% CO2 with 95% humidity. The cells were examined under a microscope on a daily

basis, and the medium was renewed every 2 days. Cells were passaged at 70% confluence using 0.25% trypsin, 0.53 mM EDTA solution (Corning).

Human tumor samples

Following informed consent, tissue was collected and stored in Dulbecco's Modified Eagle Medium (DMEM; Gibco) containing 50 μg/mL Gentamicin (Sigma), and gently scraped to liberate urothelial cells. The procedure was approved by the Pennsylvania State University Institutional Review Board (PSU IRB# STUDY00008190). The cell suspension was combined with an equal volume of Optiprep Density Gradient Medium (30%; Sigma). Following thorough mixing, cells were overlaid with keratinocyte serum-free growth medium (KSFM; Gibco) and centrifuged at 800 x g for 15 minutes at 4 degrees C in a Sorvall ST8R refrigerated centrifuge (Thermo Scientific). Interphase containing urothelial cells was transferred to a 15 ml conical vial (Falcon) containing KSFM. This cell suspension was subsequently centrifuged. Following aspiration of the supernatant, the cell pellet was suspended in KSFM growth medium at a plating density between 10,000 and 50,000 cells/cm^2.

Microtumor Formation and Culture in Matrigel

Microtumors were generated using a self-assembly process based on a previously developed 3D culture technique for breast cancer cells.[27] Cells were stained using CellTracker Green CMFDA (Invitrogen) at a concentration of 20 μM in PBS for 30 minutes, then allowed to recover for at least 3 hours before detaching for spheroid formation. Growth factor-reduced Matrigel (Corning) was diluted to 8 mg/mL in chilled, complete culture medium. Fluorescent beads (Spherotech) were then added at a volume ratio of 1:10,000 to label the Matrigel for imaging. 40 μL labeled Matrigel was applied to each well of a chilled glass-bottom 96-well plate (CellVis), which was then placed in a humidified cell incubator at 37°C, 5% CO2 for 30 min to solidify. Cells were then suspended in complete culture medium at a concentration

of 10^6 cells/mL and seeded atop the solidified Matrigel at a concentration of 10^4 cells/well. The plate was then covered and returned to the cell culture incubator for 3 days before imaging. 50 µL fresh complete culture medium was added to each well after 2 days to prevent drying during imaging.

GNR-LNA probe design and preparation

A GNR-LNA probe sequence was used to detect single cell level DLL4 mRNA expression within the microtumors. LNA probes labeled with Texas Red were obtained from Integrated DNA Technologies. Probes at 15 nM were prepared in 1x Tris-EDTA buffer. Probes were incubated for 10 minutes at room temperature with MUTAB-coated GNRs (Nanopartz) with 10 nm diameter and 29 nm length. Cells were incubated overnight with GNR-LNA probe complex to allow sufficient time for cellular uptake.

Drug treatments

DAPT was obtained from Sigma-Aldrich; DLL4, NOTCH1, and non-targeting control siRNA were purchased from Santa Cruz Biotech. DAPT was dissolved in DMSO and diluted in medium to desired concentrations for drug response testing. DAPT was added after microtumor self-assembly, 48 hours before imaging. All siRNAs were diluted in serum-free medium and mixed with Hiperfect transfection reagent (Qiagen) according to the manufacturer's instructions. Transfection was performed in monolayer culture for 24 hours prior to microtumor self-assembly.

Imaging and Data analysis

3D images stacks were taken using confocal microscopy (Leica SP8) and reconstructed using open-source software (NIH ImageJ). Invasion depth was measured as the distance from the gel-medium interface to the leading edge of each spheroid. To analyze fluorescence intensity, 3D images containing

individual spheroids were imported into MATLAB and binarized, and intensity was calculated as the ratio of active pixels for the probe channel to the number of active pixels for the cell stain channel.

Statistical Analysis

Invasiveness and DLL4 mRNA expression were compared using Kruskal-Wallis and one-way ANOVA tests with Tukey-Kramer post-tests to analyze invasion depth and fluorescence intensity, respectively, for Figures 3E and H. Two-sample *t*-tests were used for Figures 3B and S4B. Statistical analysis was performed using MATLAB statistics toolbox (Mathworks). A p value less than 0.05 was considered statistically significant.

Results

Urothelial carcinoma cells self-organize into microtumors

Urothelial carcinomas of the kidney, ureter, and bladder are characterized by the tendency of the tumor being confined in the mucosa or invading through the basement membrane (primary tumor stages Tis and pTa) and lamina propria (stage T1) and eventually into the muscularis propria (stage T2; Figure 1A). To mimic the lumen/tumor/basement membrane structure, we developed a 3D microtumor invasion model through self-assembly of urothelial carcinoma cells on ECM, such as Matrigel.[27] The cancer cells migrated and aggregated on the ECM to form microtumor structures (Supplementary Information Figure S1A-B and Movie S1). Hundreds of microtumor structures could be developed simultaneously with an appropriate cell seeding density and ECM properties (Supplementary Information Figure S1C). The tumor-on-gel self-assembly was implemented in standard 96-well plates. The microtumor assay is compatible with bladder cancer cells and other urothelial carcinoma cells (Supplementary Information Figure S1-2). Flat carcinoma and papillary carcinoma-like microtumors with infiltrative and finger-like

protrusions that recapitulate the diversity of bladder cancer invasion were observed (Supplementary Information Figure S2).

Invasion of bladder microtumors with heterogeneous characteristics

Bladder cancer cell lines with luminal (UM-UC-1 and RT4) and basal (HT-1376) molecular signatures as well as a highly invasive bladder cancer cell line (UM-UC-3, which is not classified as either luminal or basal) were investigated to study the microtumor invasion model (Figure 1B).[18] Microtumors were allowed to form and invade the ECM for 72 hours. Confocal imaging with 3D reconstruction was performed to visualize the invading microtumors and estimate the invasion depth (Figure 1C). For cell types with a luminal signature, such as UM-UC-1 (grade 2) and RT4 (grade 1-2),[28] the microtumors had a low-to-medium tendency to invade Matrigel, which is composed of basement membrane matrix. In contrast, HT-1376 (grade 3)[28] exhibited significantly higher invasiveness than UM-UC-1 and RT4. Furthermore, UM-UC-3 displayed highly aggressive behavior, with invading sprouts and detached cells and cell clusters from the microtumors.

The distribution of invasion depth was analyzed for several bladder cancer cell lines (Figure 1D). UM-UC-1 microtumors did not display any observable invasiveness beyond contact mechanics.[29] In contrast, the other cell lines displayed substantial heterogeneity in the invasive behaviors. A small portion of RT4 microtumors invaded over 100 μm while the majority of microtumors invaded less than 50 μm. Data analysis suggests a distorted Gaussian distribution or a bimodal distribution, implying a heterogeneous subpopulation of cancer cells may exist among the microtumors formed by the individual cell line. Similarly, small subpopulations of HT-1376 microtumors appeared capable of invading the ECM with higher frequency than the luminal cell lines. The majority of UM-UC-3 microtumors were highly non-spheroidal and invasive. For the cell lines HT-1376 and UM-UC-3, both the frequency of invading

microtumors and the invasion depths were increased, representing a spectrum of invasiveness among these cell lines. These results are in excellent agreement with previous investigations of bladder cancer cell behaviors using in vivo and ex vivo bladder cancer models.[28,30–32]

Single cell analysis of invading microtumors using the GNR-LNA biosensor

Next, we investigated the invasion mechanism of microtumors using a GNR-LNA biosensor. In particular, we investigated the expression of DLL4 mRNA as it is associated with the formation of leader cells during epithelial wound healing.[25,26] The GNR-LNA biosensors were internalized by the cells and detected the target mRNA by the displacement reaction between the target mRNA and the GNR (Figure 2A).[20–22] When used in combination with 3D confocal imaging, this biosensor allows us to study the spatiotemporal distribution of mRNA expression within individual microtumors. An LNA sequence for targeting DLL4 mRNA was previously designed and optimized.[33] Probe sequences targeting β-actin and GAPDH mRNA were included as the positive control and a random sequence was chosen as the negative control.[13,34] In the experiment, β-actin and GAPDH probes exhibited little variation in the expression (volume average) among the microtumors and the expressions were also relatively uniform within individual microtumors (Figure 2B). The random probes, in contrast, maintained a low background signal. Interestingly, the bulk expression of DLL4 was heterogeneous among different microtumors, and non-uniform distribution of DLL4 expression was observed within some of microtumors (Figure 2C). Specifically, the cells displayed a high level of DLL4 mRNA at the leading front in some microtumors (Supplementary Information Movie S2). These results suggest DLL4 is spatially coordinated in bladder microtumors.

NOTCH1-DLL4 signaling is involved in the collective invasion of bladder cancer cells

The expression of DLL4 mRNA has been associated with the formation of leader cells in epithelial wound healing and endothelial tip cells during angiogenesis.[23–26] To study the role of DLL4 in the formation of invasive leader cells and bladder cancer invasion, 3D reconstruction was applied to evaluate the DLL4 expression in invading microtumors. HT-1376, which has a moderate invasiveness and form uniform spheroids, was chosen as the model cell. The expression of DLL4 mRNA was upregulated in HT-1376 cells at the leading front of invading microtumors (Figure 3A). To characterize this observation, we measured the level of DLL4 at day 3 after cell seeding and tracked the migration of microtumors over 72 hours (day 6 after cell seeding). Microtumors with a high level of DLL4 at the leading front generally invaded a greater depth compared to microtumors with a low level of DLL4 (Figure 3B). The data revealed a positive correlation between the level of DLL4 at the leading front and invasion depth (Supplementary Information Figure S3A), suggesting a potential role of DLL4 in bladder cancer invasion.

NOTCH1 is a receptor of DLL4 and is associated with the progression of bladder cancer.[35] In particular, NOTCH1 is suggested as a tumor suppressor, and inhibition of NOTCH1 signaling promotes bladder cancer progression. Therefore, we investigated the influence of NOTCH1-DLL4 signaling on the invasion of bladder microtumors. HT-1376 microtumors were treated with DAPT, a γ-secretase inhibitor, which prevents the cleavage of the Notch intracellular domain and therefore inhibits Notch activation. HT-1376 cells were treated with DAPT prior to microtumor self-assembly (Figure 3C and Supplementary Information Figure S3B-C). Upregulation of DLL4 at the leading edge was observed in microtumors treated with DAPT (Figure 3D). This observation is consistent with the inhibitory role of NOTCH1 on DLL4.[36] Interestingly, invasion depth measurements indicated that increasing concentrations of DAPT increased the median invasion depth (Figure 3E). The effect of NOTCH1-DLL4 signaling on bladder cancer invasion was further investigated by RNA interference (Supplementary

Information Figure S3D-F). HT-1376 cells were treated with NOTCH1 and DLL4 siRNA before seeding, and microtumor invasion was monitored in the same manner. In agreement with the DAPT data, transient knockdown of NOTCH1 enhanced the expression of DLL4 and increased the invasion depth (Figure 3F-H). In contrast, DLL4 siRNA reduced DLL4 expression and significantly attenuated the invasion of microtumors relative to control siRNA (Figure 3G-I). These results collectively support the inhibitory role of NOTCH1 on DLL4 expression and bladder tumor invasion.

Characterization of patient derived primary tumor cells

To evaluate the involvement of DLL4 in patient samples and demonstrate personalized analysis using the 3D microtumor invasion assay, we incorporated fresh human clinical specimens collected from patients diagnosed with bladder cancer. We optimized a protocol for studying patient-derived tumor cells and functionally characterized the invasiveness of the sample. In the protocol, the cells were stained and the GNR-LNA biosensor targeting DLL4 mRNA was applied for single cell gene expression analysis. Submicron fluorescent particles were embedded in the ECM to track the invasion depth of the microtumor. Figure 4A shows a microtumor generated by a high-grade papillary urothelial carcinoma sample obtained from TURBT. Similar to the experiments using bladder cancer cell lines, the primary cancer cells self-assembled on the ECM. The cells formed a single microtumor of ~500 μm diameter in each well, and the morphology of the microtumor was similar to the high-grade UM-UC-3 cells (Figure 4B-C). Some of the cells invaded aggressively as protruding structures sprouting from the microtumor (Figure 4D). The microtumor also exhibited many small aggregates detaching and penetrating collectively and individually into the ECM over time (Figure 4E). In agreement with the experiments using cell lines, DLL4 expression was upregulated in both the main microtumor and detached cell aggregates. The distribution of DLL4 was non-uniform among the aggregates (Supplementary Information Fig. S4A). In particular, the majority of invading cell aggregates had one or more DLL4

expressing cells while the other cells in the aggregate exhibited a low or undetectable level of DLL4 mRNA. The average DLL4 expression is comparable between cells at the boundary of the main spheroid and the detached cell aggregates (Supplementary Information Fig. S4B). Interestingly, the invasion depth of cell aggregates with DLL4 expressing cells (n=13) is significantly higher than cell aggregates without (n = 4) DLL4 expressing cells (Supplementary Information Fig. S4C). These results further support the correlation between increased DLL4 expression and invasive behavior and demonstrate the importance of molecular heterogeneity within a tumor sample.

Discussion

In this study, we demonstrated a 3D microtumor assay for assessing the phenotypic heterogeneity of bladder cancer cell invasion at multiple levels. First, our model was designed to analyze the capability of cancer cells to degrade and penetrate the type of extracellular matrix found in the basement membrane. Interactions with healthy urothelial cells, fibroblasts, and other basement membrane components that could affect invasion are not considered. Furthermore, the basement membrane is typically less than 100 nm thick, so significant invasion in our model does not imply that these cells would invade the same distance when crossing the basement membrane and invading the lamina propria in vivo. Rather, cells that have a high potential to penetrate the simulated basement membrane ECM in our model are expected to be more likely to cross the basement membrane in vivo, which represents a crucial first step in bladder cancer invasion. The applicability of this invasion assay for characterizing the invasive subtypes within cellular populations is supported by our use of several established bladder cancer cell lines. While all cell lines exhibited considerable mobility on the ECM and self-assembled into microtumor structures, some cell lines, including the basal subtype HT-1376 and invasive non-type UM-UC-3 lines, exhibited more aggressive behavior in regards to invading the ECM compared to luminal cells. The data are in good agreement with previous ex vivo and in vivo studies,[28,30–32] supporting the use of the model for

characterizing the invasiveness of bladder cancer. The results indicate that microtumor invasiveness is a distinct feature compared to cell mobility on a 2D substrate, underscoring the importance of 3D invasion assays in studying bladder cancer invasiveness. Second, the microtumor invasion assay captured the molecular heterogeneity within an individual cell line, thus identifying subpopulations with enhanced invasive capabilities. Unlike conventional techniques, such as the hanging drop method, self-assembly of bladder cancer cells on ECM can create hundreds of microtumors in each well simultaneously, allowing the molecular diversity of subpopulations to manifest. Compared with other tumor organoid models,[10–12] the on-gel microtumor self-assembly approach is amendable with GNR-LNA biosensors for single cell analysis and genetic modification (Supplementary Information Figure S5). Third, we investigated the coordination within the invasive microtumors and observed the formation of invasive leader cells in invading microtumors. In traditional 2D migration assays, such as the monolayer wound healing assay, emerging evidence supports a "leader" cell phenotype that positions at the leading edge, and we have previously demonstrated that DLL4 mRNA is a molecular signature of leader cells.[26] Invasive leader cells with basal features were reported in breast cancer invasion; however, the leader-follower organization remains poorly understood in the invasion of other cancer types.[13,19] By incorporating a GNR-LNA biosensor, we observed DLL4 upregulation in the leading front of microtumors and a positive correlation between DLL4 expression and invasion depth. These results provide evidence in the involvement of invasive leader cells in the organization of bladder cancer invasion.

Our results suggest NOTCH1-DLL4 signaling regulates the invasion of bladder cancer. DLL4, which is a ligand for NOTCH1 receptor, plays an important role in angiogenesis and wound healing.[23–26] Previous studies have noted a correlation between DLL4 expression and progression of several cancer types.[37,38] The mechanistic basis of anti-DLL4 therapy, however, is only partially understood, and multiple

mechanisms have been proposed for anti-DLL4 therapy.[39] For instance, DLL4 is a target of therapy based on anti-tumor angiogenesis and is associated with proliferation and differentiation of cancer stem cells [40]. In our experiment, DLL4 was upregulated in invasive microtumors formed by cell lines and patient derived cancer cells. A correlation was observed between DLL4 expression and the invasion depth of the microtumor. Our results also indicated that NOTCH1 negatively regulates DLL4 during microtumor invasion. NOTCH1 inhibition by DAPT or siRNA enhanced the expression of DLL4 and the invasiveness of the microtumors. In contrast, transient knockdown of DLL4 resulted in a reduction of DLL4 expressing cells at the leading front and the invasiveness of the microtumors (Figure 3). These results collectively suggest DLL4 inhibition may contribute to the anti-cancer effect by attenuating the invasive subpopulation and invasive leader cells. In the future, investigation should be performed to elucidate the mechanistic function of DLL4 in tumor invasion. Clinical studies will be required to decipher the role of DLL4 in the formation of invasive leader cells and evaluate the potential of anti-invasion therapy by targeting DLL4.

Pathologic interpretation of tissue specimens has been the major approach for bladder cancer staging and classification for over a century. Since it is difficult to predict the clinical outcome of bladder cancer patients, the 3D invasion assay may serve as a phenotypic surrogate assay for characterizing the invasiveness of patient tumor samples. Our results show that the 3D invasion assay and the GNR-LNA biosensor are compatible with primary cancer cells obtained from TURBT. In the future, the inclusion of additional simulated tissue layers and incorporation of stromal cells will be required to better evaluate the interactions between the tumor and the microenvironment. The protocol for isolating patient-derived tumor cells should also be further optimized to improve the efficiency and capture other stromal cells. Furthermore, molecular subtyping with high-throughput sequencing techniques and bioinformatics will provide useful information for guiding the treatment of muscle invasive bladder cancer.[5–7] The collection

of these technologies will potentially enable a comprehensive approach for guiding personalized treatment of bladder cancer in the future.

Conclusion

Using established cell lines and human clinical specimens derived from TURBT, this study demonstrated a 3D microtumor approach along with a single cell biosensor that overcomes some limitations of existing cancer models by targeting the invasive subpopulation. The microtumor approach can be applied for investigating cancer invasion mechanisms and for guiding treatment options for bladder cancer patients.

Acknowledgements

This work is supported by the Penn State Grace Woodward Grant and NSF Biophotonics Program (1802947).

Supplementary information

Figure

References

(1) Sanli, O.; Dobruch, J.; Knowles, M. A.; Burger, M.; Alemozaffar, M.; Nielsen, M. E.; Lotan, Y. Bladder Cancer. *Nat. Rev. Dis. Prim.* **2017**, *3*, 17022. https://doi.org/10.1038/nrdp.2017.22.

(2) Chen, C.; Qi, X. J.; Cao, Y. W.; Wang, Y. H.; Yang, X. C.; Shao, S. X.; Niu, H. T. Bladder Tumor Heterogeneity: The Impact on Clinical Treatment. *Urol. Int.* **2015**, *95* (1), 1–8. https://doi.org/10.1159/000370165.

(3) Warrick, J. I.; Sjödahl, G.; Kaag, M.; Raman, J. D.; Merrill, S.; Shuman, L.; Chen, G.; Walter, V.; DeGraff, D. J. Intratumoral Heterogeneity of Bladder Cancer by Molecular Subtypes and Histologic Variants. *Eur. Urol.* **2018**, 0–4. https://doi.org/10.1016/j.eururo.2018.09.003.

(4) Knowles, M. A.; Hurst, C. D. Molecular Biology of Bladder Cancer: New Insights into Pathogenesis and Clinical Diversity. *Nat. Rev. Cancer* **2015**, *15* (1), 25–41. https://doi.org/10.1038/nrc3817.

(5) Cancer Genome Atlas Research Network, T. Comprehensive Molecular Characterization of Urothelial Bladder Carcinoma. *Nature* **2014**, *507* (7492), 315–322. https://doi.org/10.1038/nature12965.

(6) Choi, W.; Porten, S.; Kim, S.; Willis, D.; Plimack, E. R.; Roth, B.; Cheng, T.; Tran, M.; Lee, I.; Melquist, J.; et al. Identification of Distinct Basal and Luminal Subtypes of Muscle- Invasive Bladder Cancer with Different Sensitivities to Frontline Chemotherapy. *Cancer Cell* **2014**, *25* (2), 152–165. https://doi.org/10.1016/j.ccr.2014.01.009.Identification.

(7) Damrauer, J. S.; Hoadley, K. A.; Chism, D. D.; Fan, C.; Tignanelli, C. J.; Wobker, S. E.; Yeh, J. J.; Milowsky, M. I.; Iyer, G.; Parker, J. S.; et al. Intrinsic Subtypes of High-Grade Bladder Cancer Reflect the Hallmarks of Breast Cancer Biology. *Proc. Natl. Acad. Sci. U. S. A.* **2014**, *111* (8), 3110–3115. https://doi.org/10.1073/pnas.1318376111.

(8) Hovelson, D. H.; Udager, A. M.; McDaniel, A. S.; Grivas, P.; Palmbos, P.; Tamura, S.; Lazo de

la Vega, L.; Palapattu, G.; Veeneman, B.; El-Sawy, L.; et al. Targeted DNA and RNA Sequencing of Paired Urothelial and Squamous Bladder Cancers Reveals Discordant Genomic and Transcriptomic Events and Unique Therapeutic Implications. *Eur. Urol.* **2018**, *74* (6), 741–753. https://doi.org/10.1016/j.eururo.2018.06.047.

(9) Thomsen, M. B. H.; Nordentoft, I.; Lamy, P.; Vang, S.; Reinert, L.; Mapendano, C. K.; Høyer, S.; Ørntoft, T. F.; Jensen, J. B.; Dyrskjøt, L. Comprehensive Multiregional Analysis of Molecular Heterogeneity in Bladder Cancer. *Sci. Rep.* **2017**, *7* (1), 1–9. https://doi.org/10.1038/s41598-017-11291-0.

(10) Lee, S. H.; Hu, W.; Matulay, J. T.; Silva, M. V.; Owczarek, T. B.; Kim, K.; Chua, C. W.; Barlow, L. M. J.; Kandoth, C.; Williams, A. B.; et al. Tumor Evolution and Drug Response in Patient-Derived Organoid Models of Bladder Cancer. *Cell* **2018**, *173* (2), 515-528.e17. https://doi.org/10.1016/j.cell.2018.03.017.

(11) Mullenders, J.; de Jongh, E.; Brousali, A.; Roosen, M.; Blom, J. P. A.; Begthel, H.; Korving, J.; Jonges, T.; Kranenburg, O.; Meijer, R.; et al. Mouse and Human Urothelial Cancer Organoids: A Tool for Bladder Cancer Research. *Proc. Natl. Acad. Sci.* **2019**, *116* (10), 4567–4574. https://doi.org/10.1073/pnas.1803595116.

(12) Ringuette Goulet, C.; Bernard, G.; Chabaud, S.; Couture, A.; Langlois, A.; Neveu, B.; Pouliot, F.; Bolduc, S. Tissue-Engineered Human 3D Model of Bladder Cancer for Invasion Study and Drug Discovery. *Biomaterials* **2017**, *145*, 233–241. https://doi.org/10.1016/j.biomaterials.2017.08.041.

(13) Dean, Z. S.; Elias, P.; Jamilpour, N.; Utzinger, U.; Wong, P. K. Probing 3D Collective Cancer Invasion Using Double-Stranded Locked Nucleic Acid Biosensors. *Anal. Chem.* **2016**, *88* (17), 8902–8907. https://doi.org/10.1021/acs.analchem.6b02608.

(14) Liu, L.; Duclos, G.; Sun, B.; Lee, J.; Wu, A.; Kam, Y.; Sontag, E. D.; Stone, H. A.; Sturm, J. C.; Gatenby, R. A.; et al. Minimization of Thermodynamic Costs in Cancer Cell Invasion. *Proc. Natl.*

Acad. Sci. U. S. A. **2013**, *110* (5), 1686–1691. https://doi.org/10.1073/pnas.1221147110.

(15) Li, Y. H.; Zhu, C. A Modified Boyden Chamber Assay for Tumor Cell Transendothelial Migration in Vitro. *Clin. Exp. Metastasis* **1999**, *17* (5), 423–429. https://doi.org/10.1023/A:1006614232388.

(16) Bersini, S.; Jeon, J. S.; Dubini, G.; Arrigoni, C.; Chung, S.; Charest, J. L.; Moretti, M.; Kamm, R. D. A Microfluidic 3D Invitro Model for Specificity of Breast Cancer Metastasis to Bone. *Biomaterials* **2014**, *35* (8), 2454–2461. https://doi.org/10.1016/j.biomaterials.2013.11.050.

(17) Cheung, K. J.; Ewald, A. J. Invasive Leader Cells: Metastatic Oncotarget. *Oncotarget* **2014**, *5* (6), 1390–1391. https://doi.org/10.18632/oncotarget.1870.

(18) Warrick, J. I.; Walter, V.; Yamashita, H.; Chung, E.; Shuman, L.; Amponsa, V. O.; Zheng, Z.; Chan, W.; Whitcomb, T. L.; Yue, F.; et al. FOXA1, GATA3 and PPARIγ Cooperate to Drive Luminal Subtype in Bladder Cancer: A Molecular Analysis of Established Human Cell Lines. *Sci. Rep.* **2016**, *6* (December), 1–15. https://doi.org/10.1038/srep38531.

(19) Cheung, K. J.; Gabrielson, E.; Werb, Z.; Ewald, A. J. Collective Invasion in Breast Cancer Requires a Conserved Basal Epithelial Program. *Cell* **2013**, *155* (7), 1639–1651. https://doi.org/10.1016/j.cell.2013.11.029.

(20) Wang, S.; Xiao, Y.; Zhang, D. D.; Wong, P. K. A Gapmer Aptamer Nanobiosensor for Real-Time Monitoring of Transcription and Translation in Single Cells. *Biomaterials* **2018**, *156*, 56–64. https://doi.org/10.1016/j.biomaterials.2017.11.026.

(21) Wang, S.; Riahi, R.; Li, N.; Zhang, D. D.; Wong, P. K. Single Cell Nanobiosensors for Dynamic Gene Expression Profiling in Native Tissue Microenvironments. *Adv. Mater.* **2015**, *27* (39), 6034–6038. https://doi.org/10.1002/adma.201502814.

(22) Riahi, R.; Wang, S.; Long, M.; Li, N.; Chiou, P. Y.; Zhang, D. D.; Wong, P. K. Mapping Photothermally Induced Gene Expression in Living Cells and Tissues by Nanorod-Locked Nucleic Acid Complexes. *ACS Nano* **2014**, *8* (4), 3597–3605. https://doi.org/10.1021/nn500107g.

(23) Hellström, M.; Phng, L. K.; Hofmann, J. J.; Wallgard, E.; Coultas, L.; Lindblom, P.; Alva, J.; Nilsson, A. K.; Karlsson, L.; Gaiano, N.; et al. Dll4 Signalling through Notch1 Regulates Formation of Tip Cells during Angiogenesis. *Nature* **2007**, *445* (7129), 776–780. https://doi.org/10.1038/nature05571.

(24) Wang, S.; Sun, J.; Xiao, Y.; Lu, Y.; Zhang, D. D.; Wong, P. K. Intercellular Tension Negatively Regulates Angiogenic Sprouting of Endothelial Tip Cells via Notch1-Dll4 Signaling. *Adv. Biosyst.* **2017**, *1* (1–2), 1–23. https://doi.org/10.1002/adbi.201600019.

(25) Xiao, Y.; Riahi, R.; Torab, P.; Zhang, D. D.; Wong, P. K. Collective Cell Migration in 3D Epithelial Wound Healing. *ACS Nano* **2019**, *13*, 1204–1212. https://doi.org/10.1021/acsnano.8b06305.

(26) Riahi, R.; Sun, J.; Wang, S.; Long, M.; Zhang, D. D.; Wong, P. K. Notch1-Dll4 Signalling and Mechanical Force Regulate Leader Cell Formation during Collective Cell Migration. *Nat. Commun.* **2015**, *6*, 1–11. https://doi.org/10.1038/ncomms7556.

(27) Lee, G. Y.; Kenny, P. A.; Lee, E. H.; Bissell, M. J. Three-Dimensional Culture Models of Normal and Malignant Breast Epithelial Cells. *Nat. Methods* **2007**, *4* (4), 359–365. https://doi.org/10.1038/nmeth1015.

(28) Zuiverloon, T. C. M.; De Jong, F. C.; Costello, J. C.; Theodorescu, D. Systematic Review: Characteristics and Preclinical Uses of Bladder Cancer Cell Lines. *Bl. Cancer* **2018**, *4* (2), 169–183. https://doi.org/10.3233/BLC-180167.

(29) Luo, Y.; Zhu, Y. T.; Ma, L. L.; Pang, S. Y.; Wei, L. J.; Lei, C. Y.; He, C. W.; Tan, W. L. Characteristics of Bladder Transitional Cell Carcinoma with E-Cadherin and N-Cadherin Double-Negative Expression. *Oncol. Lett.* **2016**, *12* (1), 530–536. https://doi.org/10.3892/ol.2016.4671.

(30) Fujiyama, C.; Jones, A.; Fuggle, S.; Bicknell, R.; Cranston, D.; Harris, A. L. Human Bladder Cancer Invasion Model Using Rat Bladder in Vitro and Its Use to Test Mechanisms and

Therapeutic Inhibitors of Invasion. *Br. J. Cancer* **2001**, *84* (4), 558–564. https://doi.org/10.1054/bjoc.2000.1641.

(31) Jäger, W.; Moskalev, I.; Janssen, C.; Hayashi, T.; Gust, K. M.; Awrey, S.; Black, P. C. Minimally Invasive Establishment of Murine Orthotopic Bladder Xenografts. *J. Vis. Exp.* **2014**, No. 84, 1–10. https://doi.org/10.3791/51123.

(32) Wang, S.; Sun, J.; Zhang, D. D.; Wong, P. K. A Nanobiosensor for Dynamic Single Cell Analysis during Microvascular Self-Organization. *Nanoscale* **2016**, *8* (38), 16894–16901. https://doi.org/10.1039/C6NR03907C.

(33) Dean, Z. S.; Riahi, R.; Wong, P. K. Spatiotemporal Dynamics of MicroRNA during Epithelial Collective Cell Migration. *Biomaterials* **2015**, *37*, 156–163. https://doi.org/10.1016/j.biomaterials.2014.10.022.

(34) Goriki, A.; Seiler, R.; Wyatt, A. W.; Contreras-Sanz, A.; Bhat, A.; Matsubara, A.; Hayashi, T.; Black, P. C. Unravelling Disparate Roles of NOTCH in Bladder Cancer. *Nat. Rev. Urol.* **2018**, *15* (6), 345–357. https://doi.org/10.1038/s41585-018-0005-1.

(35) Fortini, M. E. Notch Signaling: The Core Pathway and Its Posttranslational Regulation. *Dev. Cell* **2009**, *16* (5), 633–647. https://doi.org/10.1016/j.devcel.2009.03.010.

(36) Patel, N. S.; Dobbie, M. S.; Rochester, M.; Steers, G.; Poulsom, R.; Le Monnier, K.; Cranston, D. W.; Li, J. L.; Harris, A. L. Up-Regulation of Endothelial Delta-like 4 Expression Correlates with Vessel Maturation in Bladder Cancer. *Clin. Cancer Res.* **2006**, *12* (16), 4836–4844. https://doi.org/10.1158/1078-0432.CCR-06-0285.

(37) Jubb, A. M.; Turley, H.; Moeller, H. C.; Steers, G.; Han, C.; Li, J. L.; Leek, R.; Tan, E. Y.; Singh, B.; Mortensen, N. J.; et al. Expression of Delta-like Ligand 4 (Dll4) and Markers of Hypoxia in Colon Cancer. *Br. J. Cancer* **2009**, *101* (10), 1749–1757. https://doi.org/10.1038/sj.bjc.6605368.

(38) Gurney, A.; Hoey, T. Anti-DLL4, a Cancer Therapeutic with Multiple Mechanisms of Action.

Vasc. Cell **2011**, *3*, 2–5. https://doi.org/10.1186/2045-824X-3-18.

(39) Kuhnert, F.; Kirshner, J. R.; Thurston, G. Dll4-Notch Signaling as a Therapeutic Target in Tumor Angiogenesis. *Vasc. Cell* **2011**, *3*, 1–8. https://doi.org/10.1186/2045-824X-3-20.

(40) Hoey, T.; Yen, W. C.; Axelrod, F.; Basi, J.; Donigian, L.; Dylla, S.; Fitch-Bruhns, M.; Lazetic, S.; Park, I. K.; Sato, A.; et al. DLL4 Blockade Inhibits Tumor Growth and Reduces Tumor-Initiating Cell Frequency. *Cell Stem Cell* **2009**, *5* (2), 168–177. https://doi.org/10.1016/j.stem.2009.05.019.

Figures

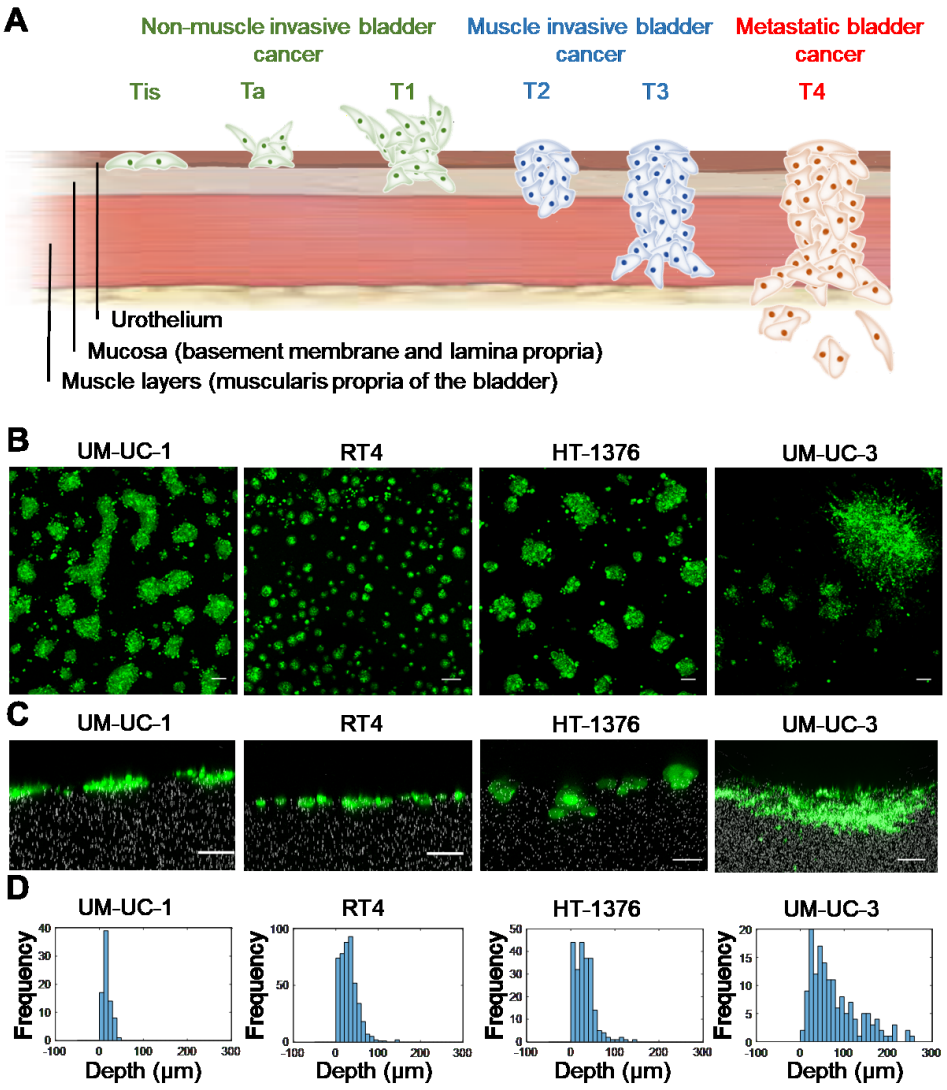

Figure 1. A microtumor model for probing bladder cancer invasion. (A) Bladder cancer staging is based on the depth of tumor invasion in relation to the inner lining of the bladder. Muscle invasive bladder cancer penetrates through the connective tissue (mucosa) and invades the muscle layer (muscularis propria). (B) Top views of 3D bladder cancer cells self-assembled on extracellular matrix and formed multifocal microtumors. Bladder cancer cells, UM-UC-1, RT4, HT-1376, and UM-UC-3, were included in the study. Scale bars, 50 μm. (C) Cross-sectional views of microtumors invading the ECM. Microtumors with infiltrative and finger-like protrusions were observed to invade collectively.

Scale bars, 50 μm. (D) Histograms of invasion depth from the gel interface to the invasion front of each spheroid. Subpopulations with enhanced invasiveness were observed in RT4, HT-1376, and UM-UC-3.

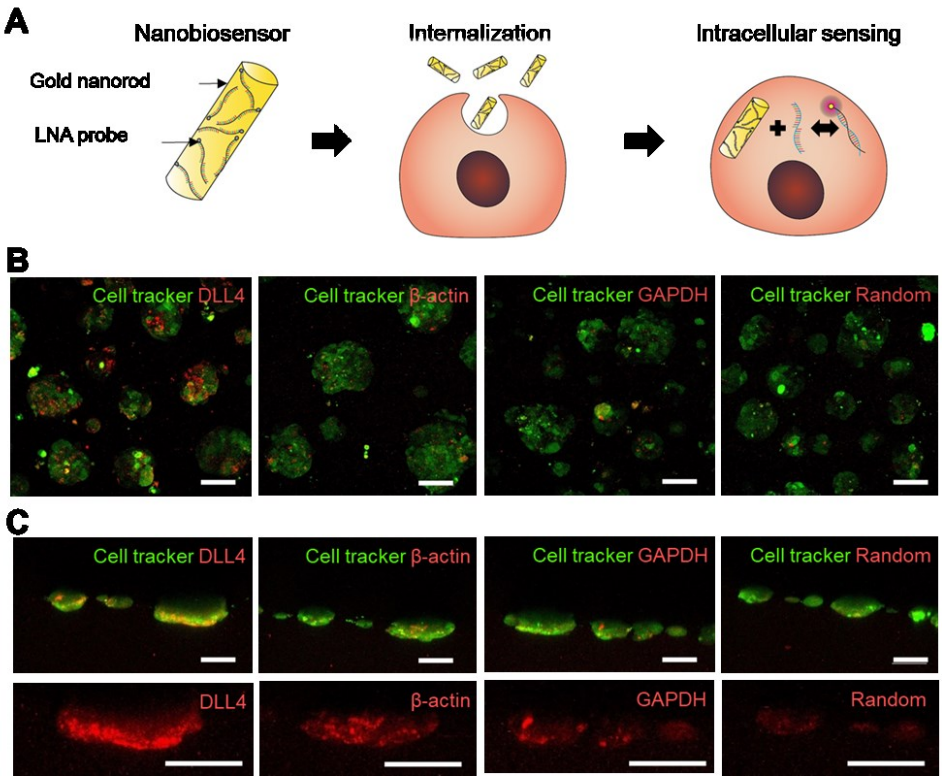

Figure 2. A gold nanorod-locked nucleic acid (GNR-LNA) biosensor for gene expression analysis in 3D microtumors. (A) Schematic of the GNR-LNA biosensor. The biosensors were internalized into live cells before self-assembly of microtumors on ECM. (B) Fluorescence images (top view) of HT-1376 microtumors with GNR-LNA probes targeting DLL4, β-actin, GAPDH, and a random sequence. Probes for β-actin and GAPDH serve as positive controls, showing uniform distribution of the targets throughout the microtumors. A random probe with a non-targeting sequence serves as the negative control. (C) Cross-sectional views of invading microtumors. Below, zoomed-in views of microtumors for illustrating the spatial gene expression profiles. DLL4 mRNA was upregulated at the leading front of invading microtumors. Scale bars, 50 μm.

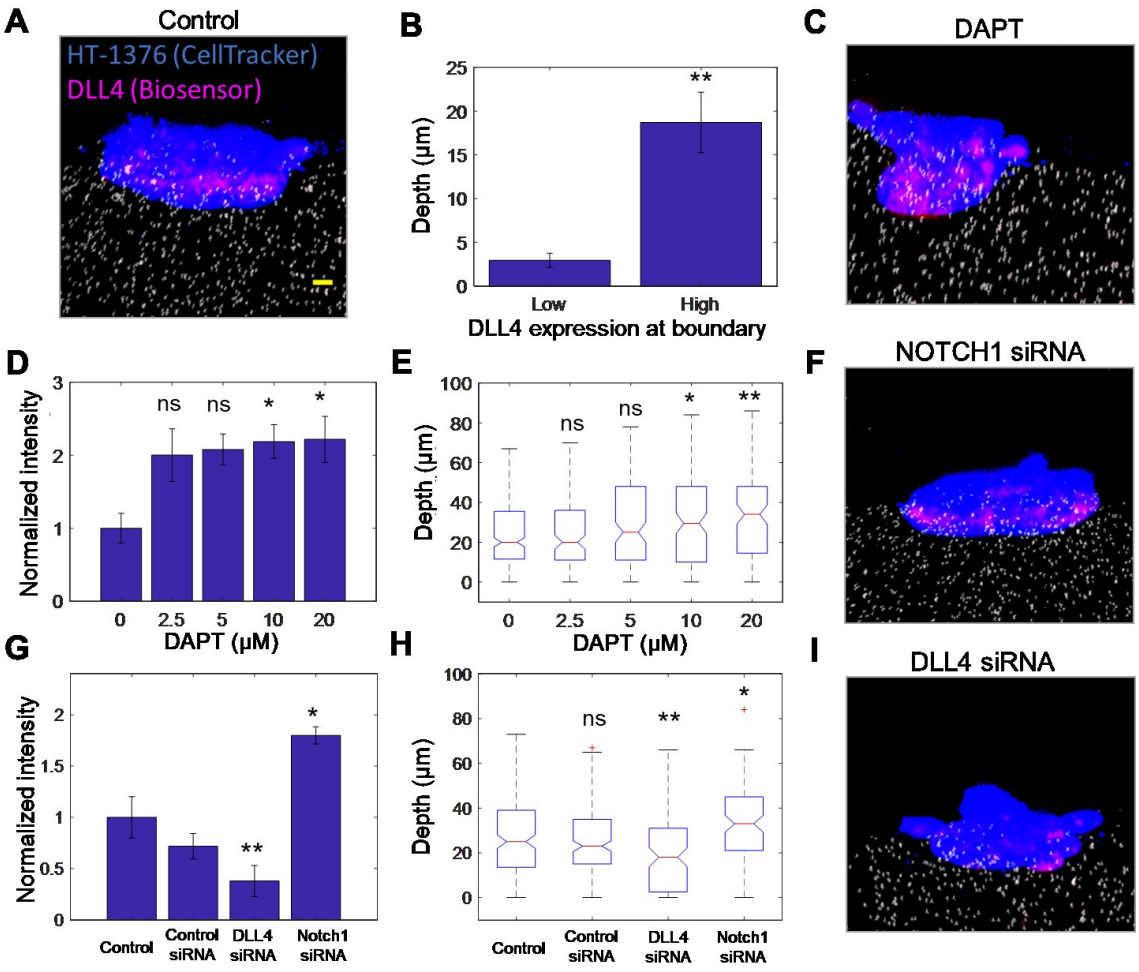

Figure 3. NOTCH1-DLL4 signaling modulates the invasion of bladder microtumors. (A,C,F,I) HT-1376 microtumors with DLL4 expressing invasive leader cells at the boundary. Scale bar, 10 μm. (B) Invasion depth of microtumors with high and low level of DLL4 expression at the boundary. Migration distance is defined as the change in invasion depth over 72 hours. Data are expressed as mean ± S.E.M. (n = 13; **p < 0.01; two-tailed unpaired Student's *t*-test). (D-E) Perturbation of Notch signaling by DAPT, a γ-secretase inhibitor, enhanced the expression of DLL4 and increased the invasion depth of microtumors. (G-H) DLL4 siRNA attenuated DLL4 expression and reduced invasion depth whereas NOTCH1 siRNA enhanced DLL4 expression and invasion depth. Transient knockdown was performed over 24 hours prior to cell seeding. (n = 5 for intensity measurements and n > 60 for depth measurements;

ns, not significant; *p < 0.05; **p < 0.01; Kruskal-Wallis ANOVA test followed by Tukey's post-hoc test).

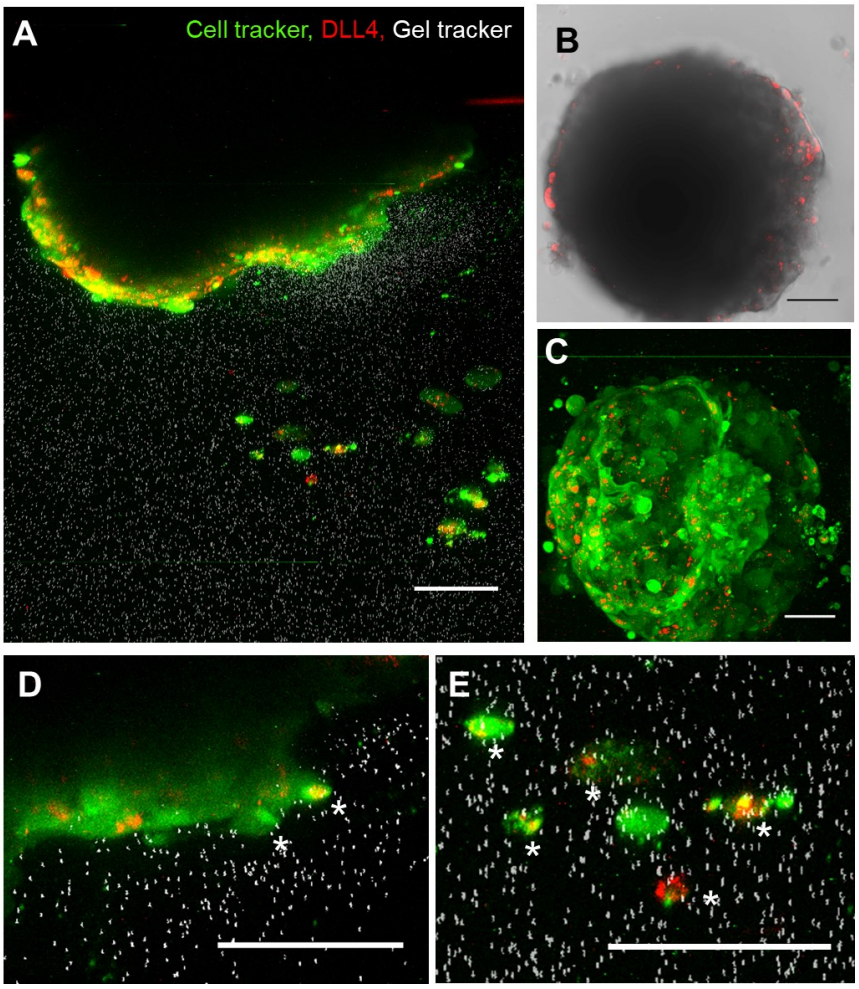

Figure 4. Invasion of patient derived cancer cells. (A) Invasion of cancer cells (cross-sectional view) from a high-grade papillary urothelial carcinoma sample obtained from transurethral resection. Fluorescent particles (white) were embedded in the ECM, and cells were stained with a CellTracker dye (green) and the GNR-LNA biosensor targeting DLL4 mRNA (red). (B-C) Bright-field and fluorescence images (top view) of the microtumor. (D-E) Zoomed-in views of cancer cells in the main microtumor and detached cells or aggregates. Red color indicates DLL4 expression in invading cells. White arrowheads indicate leader cells protruding out from the microtumor structure and white asterisks indicate invading aggregates with DLL4 expressing leader cells. Scale bars, 100 μm.

For Table of Contents Only